Power System Stabilization Using Virtual Synchronous Generator With Alternating Moment of Inertia

Jaber Alipoor, Yushi Miura, and Toshifumi Ise

***Abstract*— The virtual synchronous generator (VSG) is a control scheme applied to the inverter of a distributed generating unit to support power system stability by imitating the behavior of a synchronous machine. The VSG design of our research incorporates the swing equation of a synchronous machine to express a virtual inertia property. Unlike a real synchronous machine, the parameters of the swing equation of the VSG can be controlled in real time to enhance the fast response of the virtual machine in tracking the steady-state frequency. Based on this concept, the VSG with alternating moment of inertia is elaborated in this paper. The damping effect of the alternating inertia scheme is investigated by transient energy analysis. In addition, the performance of the proposed inertia control in stability of nearby machines in power system is addressed. The idea is supported by simulation and experimental results, which indicates remarkable performance in the fast damping of oscillations.**

***Index Terms*— Grid connected inverter, smart grid, transient stability, virtual synchronous generator (VSG), voltage source inverter.**

I. Introduction

CONVENTIONAL enormous synchronous generators (SGs) comprise rotating inertia due to their rotating parts. These generators are capable of injecting the kinetic potential energy preserved in their rotating parts to the power grid in the case of disturbances or sudden changes. Therefore, the system is robust against instability. On the other hand, penetration of distributed generating (DG) units in power systems is increasing rapidly. The most challenging issue with the inverter-based units is to synchronize the inverter with the grid and then to keep it in step with the grid even when disturbances or changes happen [1]–[3]. A power system with a big portion of inverter-based DGs is prone to instability due to the lack of adequate balancing energy injection within the proper time interval. The solution can be found in the control scheme of inverter-based DGs. By controlling the switching pattern of an inverter, it can emulate the behavior of a real synchronous machine. In the VSG concept, the power electronics interface of the DG unit is controlled in a way to exhibit a reaction similar to that of a synchronous machine to a change or disturbance. The VSG control generates amplitude, frequency, and phase angle for its terminal voltage based on its power command. Therefore, as a corollary, it can contribute to the regulation of grid voltage and frequency. In addition, synchronizing units, such as phase-locked loops, can be removed [4].

The VSG concept and application were investigated in [5] and [6]. The same concept under the title of synchronverter is described in [7]. The VSG systems addressed in [8]–[10] are designed to connect an energy storage unit to the main grid. Hesse *et al.* [11] implement a linear and ideal model of a synchronous machine to produce current reference signals for the hysteresis controller of an inverter. In this virtual synchronous machine, we also added an algorithm to compensate small disturbances and improve the quality of the grid voltage. Xiang-Zhen *et al.* [12] introduce a mechanism for voltage, frequency, and active and reactive power flow control of the VSG. The effect of the VSG on the transient response of a microgrid is addressed in a more recent publication [13]. Our research group has introduced a new VSG design, enhanced the voltage sag ride-through capability of the VSG [14], evaluated it in various voltage sag conditions [15], and finally added reactive power control to have a constant voltage at VSG terminals [16].

The quantities of the VSG, such as its output frequency and power oscillate after a change or disturbance similar to those of a synchronous machine. However, the transient condition tolerance of an inverter-based generating unit is much less than a real synchronous machine. Therefore, a VSG system may stop working redundantly due to oscillations with high amplitude after a change or disturbance. On the other hand, VSG control has an advantage in that its swing equation parameters can be adopted in real time to obtain a faster and more stable operation. This property of the VSG system is used to introduce the VSG with adoptive virtual inertia [17]. This scheme removes the oscillations and thereby, increases the reliability of the VSG unit against changes or disturbances. In this concept, the value of the virtual moment of inertia is changed based on the relative virtual angular velocity (the difference between virtual mechanical velocity generated by the VSG and grid angular frequency) and its rate of change. Therefore, we call it alternating inertia scheme. This paper goes into detail on the alternating inertia control with the objective of clarifying its damping and stabilizing effect. The damping effect is investigated by the transient energy analysis and its stabilizing performance on the nearby machines in

Manuscript received January 31, 2014; revised May 30, 2014 and July 17, 2014; accepted September 25, 2014. Date of publication October 9, 2014; date of current version April 30, 2015. Recommended for publication by Associate Editor Rolando Burgos.

The authors are with the Division of Electrical, Electronic and Information Engineering, Osaka University, Suita 565-0871, Japan (e-mail: alipoor@pe.eei.eng.osaka-u.ac.jp; miura@eei.eng.osaka-u.ac.jp; ise@eei.eng.osaka-u.ac.jp).

Color versions of one or more of the figures in this paper are available online at http://ieeexplore.ieee.org.

Digital Object Identifier 10.1109/JESTPE.2014.2362530

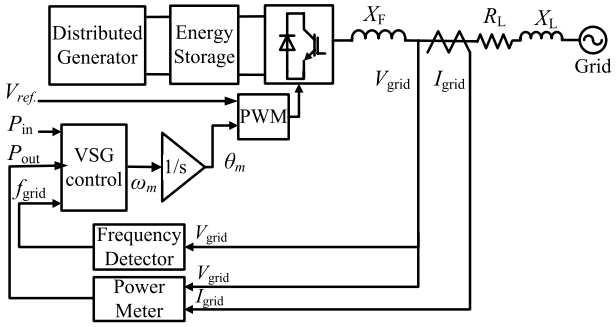

Fig. 1. Block diagram of VSG unit.

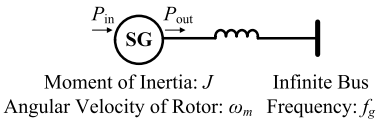

Fig. 2. Model of SG.

the power system is investigated by simulations. Finally, the performance is verified by experiments on a laboratory scale digital signal processor (DSP) controlled inverter.

The structure of the VSG system and the bang–bang control algorithm of alternating inertia control are reviewed in Sections II and III, respectively. In Section IV, the stabilizing effect of alternating inertia is clarified by transient energy analysis. In Section V, the impact of alternating inertia control on the stability of other machines in the microgrid is discussed. Experimental results are represented in Section VI. Finally, the conclusion is drawn in Section VII.

II. Virtual Synchronous Generator Structure

Fig. 1 shows the control block diagram of the VSG system. In this scheme, a distributed resource is connected to the main power system via an inverter controlled with the VSG concept. The model of SG that is used in this paper is a cylindrical-rotor-type SG connected to an infinite bus as shown in Fig. 2. The well-known swing equation of SGs is used as the heart of the VSG model

$$P_{\text{in}} - P_{\text{out}} = J\omega_m \left(\frac{d\omega_m}{dt}\right) + D\Delta\omega \tag{1}$$

where P_{in}, P_{out}, J, ω_m, and D are the input power (as same as the prime mover power in a SG), the output power of the VSG, the moment of inertia of the virtual rotor, the virtual angular velocity of the virtual rotor, and the damping factor, respectively. $\Delta\omega$ is given by $\Delta\omega = \omega_m - \omega_{\text{grid}}$, ω_{grid} being the grid frequency or the reference frequency when the grid is not available. Using voltage and current signals measured at the VSG terminals, its output power and frequency are calculated. A governor model shown in Fig. 3 is implemented to tune the input power command based on the frequency deviation. Having the essential parameters, (1) can be solved by numerical integration. By solving this equation in each control cycle, the momentary ω_m is calculated and by passing through an integrator, the virtual mechanical phase angle θ_m is produced. $V_{\text{ref.}}$ in Fig. 1 is the voltage reference

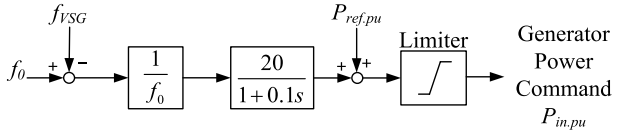

Fig. 3. Governor diagram.

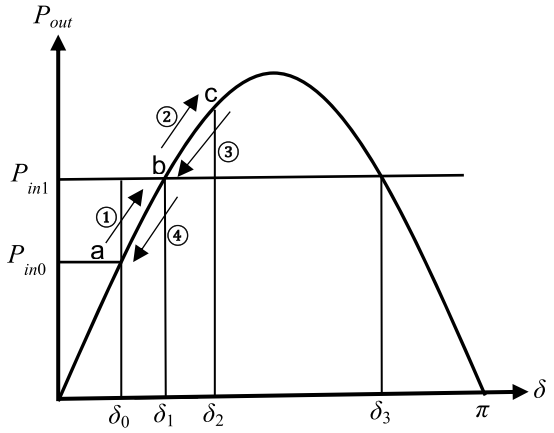

Fig. 4. Power-angle curve of a typical synchronous machine.

that determines the voltage magnitude at the inverter terminal. Implementing a controller for $V_{\text{ref.}}$ results in a regulated voltage and reactive power at the VSG terminal. However, $V_{\text{ref.}}$ is set constant in the simulations and experiments because voltage control does not affect the idea of this paper. The phase angle and the voltage magnitude reference are used as the VSG output voltage angle and magnitude commands for generating pulsewidth modulation pulses for the inverter.

The value of J together with D determines the time constant of the VSG unit. Selecting the proper value of them is a challenging issue without a routine. Mimicking a synchronous machine, J is given by $J = 2HS_{\text{base}}/\omega_0^2$ where H is the machine inertia constant, S_{base} is the base power of the machine, and ω is the system frequency. The parameter H tells that for which period of time the machine is able to supply the nominal load based solely on the energy stored in the rotating mass. The higher H, the bigger the time constant, resulting in a slower response but smaller frequency deviation after a change or disturbance. Although it depends on the machine size and power, for typical synchronous machines H varies between 2 and 10 s.

III. Bang–Bang Control Strategy of Alternating Inertia

Consider the power-angle curve of Fig. 4. After a change in system, for example, a change in prime mover power from P_{in} to P_{in1}, the operating point moves along the power curve, from point a to c and then from c to a. The machine condition during each phase of an oscillation cycle is summarized in Table I. One cycle of the oscillation consists of four segments. During each segment, the sign of the $d\omega_m/dt$ together with the sign of the relative angular velocity $\Delta\omega$ defines the acceleration or deceleration. For example, in segment ③ of Fig. 4, during transition from points c to b, both $d\omega_m/dt$ and

TABLE I
MACHINE MODES DURING OSCILLATION

Segment	$\Delta\omega$	$d\omega_m/dt$	Mode	Alternating J
a→b	$\Delta\omega > 0$	$d\omega_m/dt > 0$	Accelerating	Big value of J
b→c	$\Delta\omega > 0$	$d\omega_m/dt < 0$	Decelerating	Small value of J
c→b	$\Delta\omega < 0$	$d\omega_m/dt < 0$	Accelerating	Big value of J
b→a	$\Delta\omega < 0$	$d\omega_m/dt > 0$	Decelerating	Small value of J

$\Delta\omega$ are negative and act in the same direction; therefore, it is an acceleration period, whereas when they have opposite signs like segment ④, it is a deceleration period.

The objective is to damp frequency and power oscillation quickly by controlling the acceleration and deceleration term. The derivative of angular velocity, $d\omega_m/dt$ indicates the rate of acceleration or deceleration. Considering (1), it is observed that this rate has a reverse relation to the moment of inertia, J. Based on this fact, one can select a large value of J during acceleration phases (a to b and c to b) to reduce the acceleration and a small value of J during deceleration phases (b to c and b to a) to boost the deceleration. The big moment of inertia J_{big} and the small one J_{small} can be chosen within a wide range depending on the rated power so that the difference between J_{big} and J_{small} determines the damped power in each half-cycle of oscillation by alternating inertia. The value of J_{big} can be equal to the normal value of J. However, applying a very larger value than the normal J will result in a smaller frequency excursion at the first quarter-cycle but a sluggish response. The value of J_{small} determines the transient of the second quarter-cycle of oscillation. A very small value of J_{small} (<0.1 kgm^2) will result in a satisfactory response.

The bang–bang control strategy is summarized in Table I. During each cycle of oscillations, the value of J is switched four times. Each switching happens at the points that the sign of either $\Delta\omega$ or $d\omega_m/dt$ varies. Before the disturbance, the VSG is operating with the normal value of J. When the disturbance happens, the transition from a to b starts with $\Delta\omega > 0$ and $d\omega_m/dt > 0$. In this condition, the J_{big} is adopted. At the end of the first quarter-cycle, that is point b, the sign of $d\omega_m/dt$ changes. It means that the small value for J is adopted at this point. At point c, the sign of $\Delta\omega$ changes and J retrieves it big value. It will be the end of the first half-cycle. During the second half-cycle, the value of J is switched to the J_{small} at point b, and again at the end of one cycle at point a, J_{big} is adopted. This procedure is repeated for each cycle of oscillation until the transients are suppressed and $\Delta\omega$ equals zero at the new equilibrium point, that is, point b. A threshold for $\Delta\omega$ can be applied to avoid the chattering of J during normal operation. However, this threshold is set to zero in this paper.

Figs. 5 and 6 show simulation results of this concept. Simulations were performed on the system model of Fig. 1 with the parameters of $P_{\text{base}} = 50$ kW, $f_{\text{base}} = 60$ Hz, $R_L = 12.5\%$, $X_L = 33.0\%$, $X_F = 42.4\%$, and $D = 17$ pu. The system was subjected to increase in the VSG power reference in two steps of 70% and 30% at $t = 2$ s and $t = 8$ s, respectively. Fig. 5 shows the output power and frequency of the VSG with the fixed value of $J = 6$ kgm^2. To show the

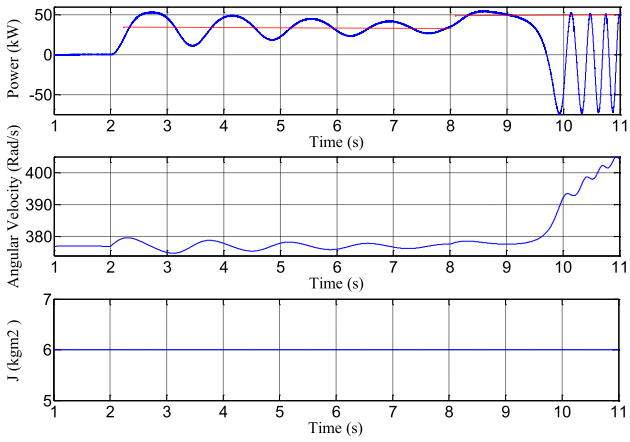

Fig. 5. Output power, virtual angular velocity, and virtual moment of inertia of VSG with fixed $J = 6$ kgm^2 and $D = 17$ pu.

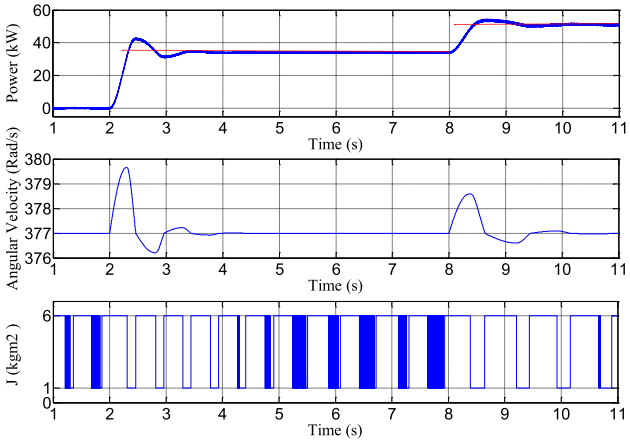

Fig. 6. Output power, virtual angular velocity, and virtual moment of inertia of VSG with alternating J: 1 and 6 kgm^2 and $D = 17$ pu.

effectiveness of the proposed idea, simulations were carried out on a weak system that VSG with fixed J cannot stabilize the frequency at the second step of power increase. Then, the control scheme of the VSG was changed to alternating inertia control, and the same scenario was applied. As it is observed in Fig. 6, alternating inertia selects the values of J out of $J_{\text{big}} = 6$ kgm^2 and $J_{\text{small}} = 1$ kgm^2. This process does not only stabilize the system, but also suppresses the frequency and power oscillations effectively.

Damping factor is an important term that defines the VSG response. An inappropriate value of damping factor may result in a high magnitude of oscillation or a sluggish response. Besides, a proper value of the damping factor in a specific working point may not end up with an acceptable response in other conditions. The alternating inertia concept allows the VSG system to exert a suitable time constant in each phase of oscillation; therefore, the importance of the damping factor in the behavior of the VSG system is reduced considerably. To assess this matter, the damping factor was changed to zero, and the same scenario was applied. Fig. 7 shows the output power and angular velocity of the VSG in this condition. It is observed that the system operates

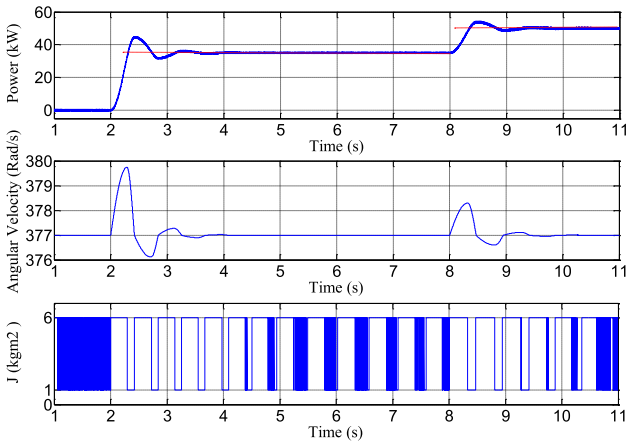

Fig. 7. Output power, virtual angular velocity, and virtual moment of inertia of VSG with alternating J: 1 and 6 kgm^2 and $D = 0$ pu.

stably, and the oscillations are eliminated by the alternating inertia idea even with a zero value for the damping factor.

IV. Stability Assessment by Energy Function Analysis

Transient stability concerns the stability of the rotor angle of synchronous machines (voltage angle in the case of VSG) after a significant disturbance. Having the advantage of not solving the nonlinear differential equations, Lyapunov direct method has become the center of attention for transient stability analysis. Consider a system expressed by a set of nonlinear differential equations of the form $\dot{\boldsymbol{x}} = \boldsymbol{F}(\boldsymbol{x})$, $\boldsymbol{x}$ being a vector of state variables. The point $\hat{\boldsymbol{x}}$ for which $\boldsymbol{F}(\hat{\boldsymbol{x}}) = 0$ is the equilibrium point of the system in state space. The solution of system state equations from initial point to the equilibrium point forms the system trajectory. The trajectory of an asymptotically stable system converges at the equilibrium point as time approaches infinity.

Based on the Lyapunov stability theorem, point $\hat{\boldsymbol{x}}$ is asymptotically stable if a continuous differentiable function $V(\boldsymbol{x})$ exists and $\dot{V}(\boldsymbol{x}) \leq 0$. In other words, the rate of change of $V(\boldsymbol{x})$ along the system trajectory is negative. The theorem is shown in Fig. 8. The $V(\boldsymbol{x})$ of Fig. 8(a) is declining during time as state variables converge to the equilibrium point that is a minimum stationary point, whereas for an unstable initial point, the value of $V(\boldsymbol{x})$ rises, and the graph diverges on the state variables plane as shown in Fig. 8(b).

Finding a candidate Lyapunov function is the next step of stability analysis. Machowski *et al.* [18] calculated the energy function through removing the damping factor, multiplying the swing equation by $\Delta\omega$, and integrating the product from the first equilibrium point, that is, point b in Fig. 4, with δ_1 and $\Delta\omega = 0$ to any point on the system transient trajectory. The resultant expression is

$$V = E_k + E_p = \frac{1}{2}\omega_0 J \Delta\omega^2 - [P_{\text{in}}(\delta - \delta_1) + b(\cos\delta - \cos\delta_1)] \tag{2}$$

where V is the system transient energy after a change or disturbance b is the amplitude of the power-angle curve, and

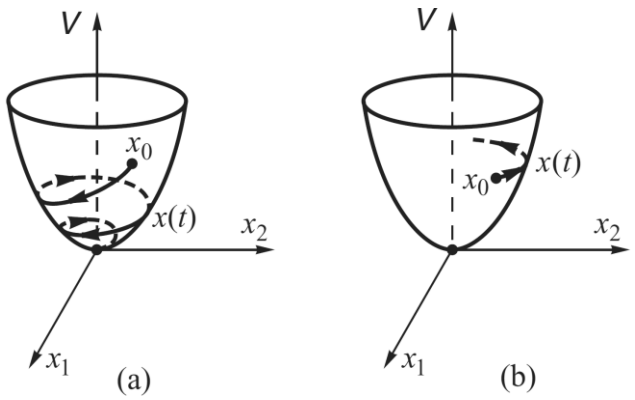

Fig. 8. Lyapunov's theorem on stability [18]. (a) Transient energy level descends in a stable case. (b) Transient energy ascends in an unstable case.

ω is the system frequency. Equation (2) has two terms. The first term, which is denoted as E_k, is the kinetic energy of the rotor of SG and virtual kinetic energy for the VSG system. The other term, E_P is the potential energy that is stored and released electromagnetically during the interaction between the electromagnetic fields of the rotor and stator of the machine. It is proved that V satisfies the Lyapunov function criteria [18]. In the case of VSG with alternating moment of inertia, only a presumption of $J > 0$ is needed.

When oscillation starts at point a of Fig. 4, $\Delta\omega$ is zero and $\delta - \delta_1$ is maximum. Therefore, $E_k = 0$ and E_P is maximum. During the transition from point a to b with a large value of J, E_k is increasing, and E_p is decreasing as $\Delta\omega$ increases and $\delta - \delta_1$ decreases. All system transient energy is converted to the kinetic form at point b with maximum $\Delta\omega$ and J_{big}. At this point, the change in the moment of inertia to the small value is applied. Therefore, the system transient energy will be decreased to a smaller value kinetic form with the same $\Delta\omega$ but J_{small}. Now, this energy will be converted to the potential form during the transition from point b to c as $\Delta\omega$ decreases and $\delta - \delta_1$ increases. Because the total energy has decreased, the amplitude of oscillation will be reduced. In other words, $\delta_2 - \delta_1$ will be much smaller than $\delta - \delta_1$. J adopts its big value at point c. However, all of the system transient energy is in potential form at this point as $\Delta\omega = 0$ and $\delta - \delta_1$ has its maximum value. Therefore, the increase in J does not increase the system energy level based on (2). This process happens in each half-cycle until $\Delta\omega$ becomes less than a desired threshold.

To see the damping effect of the alternating moment of inertia scheme, we consider the third criterion of the Lyapunov function. This criterion demands that the derivative of the energy function is negative. Thus, the system transient energy declines during time until the system state variables are settled at the equilibrium point. For a VSG with variable J by calculating the derivatives of E_k and E_p separately and considering the swing equation, the derivative of V is expressed as

$$\frac{dV}{dt} = \frac{\omega_0}{2}\Delta\omega^2\frac{dJ}{dt} - D\Delta\omega^2. \tag{3}$$

This expression must be negative to have decay in the system transient energy during oscillation. The term $-D\Delta\omega^2$

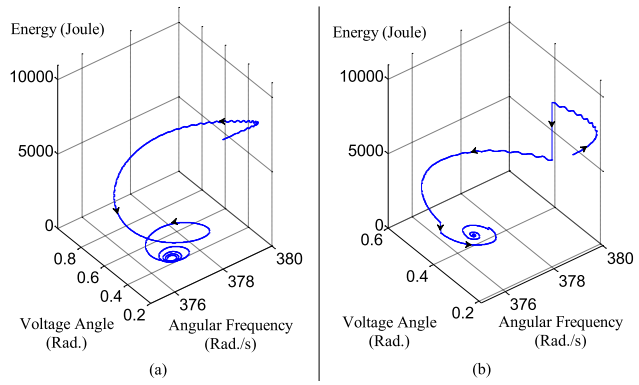

Fig. 9. Transient energy trajectory after a step change in power reference of VSG with (a) fixed moment of inertia and (b) alternating inertia.

is obviously negative for $D > 0$. Because J varies discontinuously, *dJ/dt* is approximated by its average value at the points at which J is switched. At points a and c at which J is varied from J_{small} to J_{big}, the variation of J is positive ($\Delta J = J_{\text{big}} - J_{\text{small}}$). However, *dJ/dt* is multiplied by $\Delta\omega^2$ in (3) and $\Delta\omega$ is zero at these points. It means that, the variation of J does not change the transient energy at these points. Inversely, at point b, at which J is varied from J_{big} to J_{small}, ΔJ is calculated as $J_{\text{small}} - J_{\text{big}}$, and $\Delta\omega$ has its maximum value. Therefore, the term *dJ/dt* is effective at this point and it is estimated for each half-cycle as follows:

$$\frac{dJ}{dt} \approx \frac{\Delta J}{\Delta t} = \frac{J_{\text{small}} - J_{\text{big}}}{0.5T}. \tag{4}$$

Assuming a zero damping factor D, (3) can be rewritten as

$$\frac{dV}{dt} = \frac{\omega_0}{2}\Delta\omega^2 \frac{J_{\text{small}} - J_{\text{big}}}{0.5T} < 0. \tag{5}$$

Equation (5) shows that an additional damping effect is imposed in each half-cycle by varying the value of the moment of inertia. This damping acts directly on the transient energy and cuts it to a desired level decided by the difference in the values of J. Fig. 9 shows the performance of the alternating inertia method in transient energy suppression. Simulations were performed on the system model of Fig. 1. Fig. 9(a) contains the system transient energy trajectory for a VSG with the fixed moment of inertia of 6 kgm^2 after a step increase of 1 pu in power reference. It is observed that the system transient energy declines by the damping factor as the state variables converge to the equilibrium point. When the alternating inertia scheme is applied, the transient energy drops to a desired level by applying the small J of 3 kgm^2, as shown in Fig. 9(b). By adopting a tiny J_{small}, fast decay of transient energy can be achieved, which bypasses the state variables to the stable stationary point in the first half-cycle.

There is another stationary point for the swing equation, with $\Delta\omega = 0$ and $\delta = \pi - \delta_1$ (that equals δ_3 in Fig. 4). The value of the energy function at this point is the critical transient energy. For a SG and VSG with fixed inertia, the value of energy function at the initial point of oscillation must be smaller than the critical value. However, in the case of VSG with alternating inertia scheme, any starting energy level can be reduced to nearly zero value at the end of the first quarter-cycle; therefore, the critical transient energy and thereby transient stability area will always have its maximum value, that is, $2b - \pi P_m$. Other corollaries regarding the transient stability area and the critical clearance time that can be inferred from the alternating inertia concept are forgone because of prolixity. The system kinetic, potential, and total energy in the same simulation condition as Fig. 9 are plotted in Fig. 10.

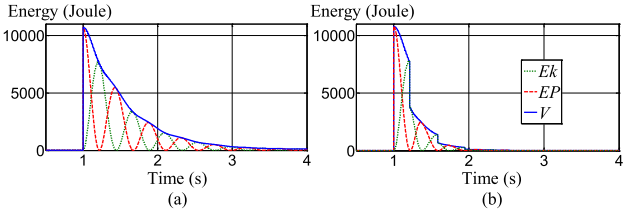

Fig. 10. Kinetic energy (Ek), potential energy (EP), and total transient energy (V) waveforms after a step increase in power reference of VSG with (a) fixed moment of inertia and (b) alternating inertia.

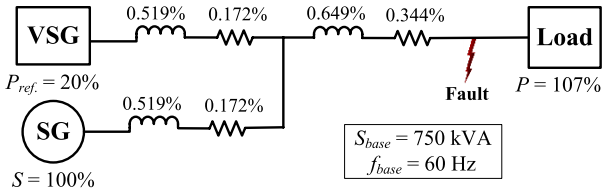

Fig. 11. VSG unit in parallel with the SG in microgrid.

V. Grid Stability Enhancement by Alternating Inertia

A. VSG in Parallel With Other Machines

In microgrid applications, an inverter-based DG works in parallel with other DGs that may include synchronous machines. Consider the islanded microgrid of Fig. 11. The VSG block has the control scheme shown in Fig. 1 with the output filter inductance of 9.7%. The objective of this part is to assess the effect of the alternating inertia scheme of the VSG on the stability of the parallel SG. To clarify the effectiveness of the idea, the capacity of the VSG unit was assumed to be 20% of the SG that is insignificant. A symmetrical fault happened at the load point at $t = 0.2$ s and lasted for 0.3 s. In this condition, the system comprising the VSG with the fixed value of moment of inertia $J = 8.445$ kgm^2 was not able to recover from the fault as shown in Fig. 12. The same scenario was applied to the system with alternating inertia of $J_{\text{big}} = 8.445$ and $J_{\text{small}} = 0.0844$ kgm^2. The waveforms of power, SG rotor angle, and angular frequency are shown in Fig. 13. As it is observed, the alternating inertia scheme improved the stability of the adjacent machine by the extra damping effect imposed on the transient energy directly.

B. VSG as an Interface Between the SG and Grid

Another configuration is shown in Fig. 14. An SG is connected to the grid/microgrid through a VSG unit. The prime mover of the SG can be a gas or diesel engine, and an

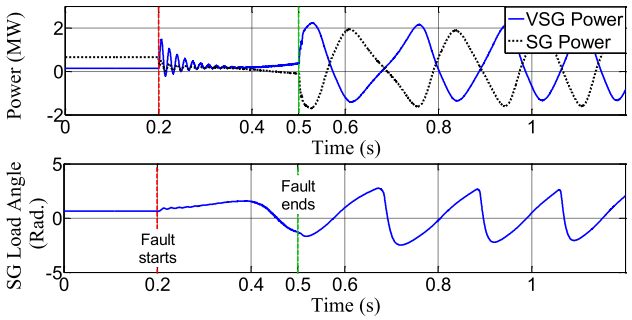

Fig. 12. VSG and SG powers and SG rotor angle waveforms of the system with fixed moment of inertia and $D = 17$ pu.

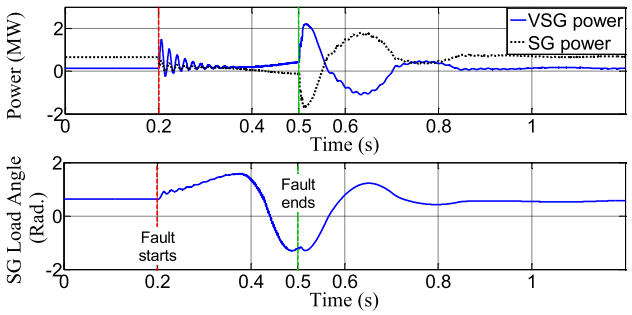

Fig. 13. VSG and SG powers and SG rotor angle waveforms of the system with alternating inertia control and $D = 0$ pu.

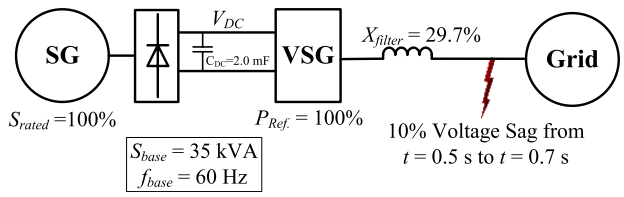

Fig. 14. SG connected to the grid via VSG unit.

inverter interface is required to correct the generated power to be injected to the grid. If the VSG unit is not robust enough, the disturbances from grid/microgrid will affect the stable operation of the SG. To assess the effect of the alternating inertia control on the stability of such systems, a symmetrical three-phase voltage sag with 10% remained voltage magnitude and the duration of 0.2 s was applied from grid side, and the performance of the system was monitored. The reference power and damping factor of the VSG were 1 and 17 pu, respectively, and a fixed inertia factor equal to 5 kgm^2 was applied. Fig. 15 shows the SG rotor angle and dc-link voltage were affected by the grid voltage sag considerably. The high-peak transient of dc-link voltage is mainly because of the oscillation of the VSG output power. The same scenario was applied to the system with the alternating inertia control with $J_{\text{big}} = 5$ and $J_{\text{small}} = 0.05$ kgm^2. To discriminate the stabilizing effect of alternating inertia as the only stabilizing effect in the system, the damping factor D was set to zero. It should be mentioned that the system with fixed inertia and a zero damping factor was unable to recover from much milder faults. As it is observed in Fig. 16, the oscillation was suppressed by the alternating

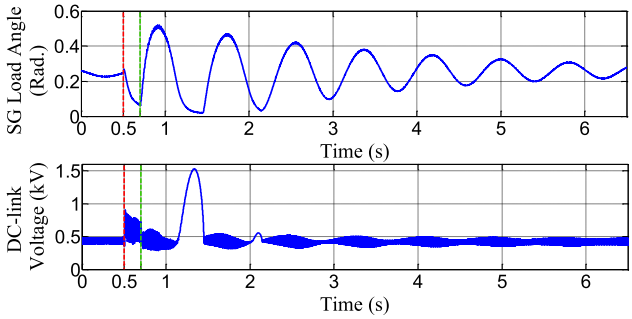

Fig. 15. SG load angle and dc-link voltage of the system of Fig. 14 containing VSG with fixed moment of inertia.

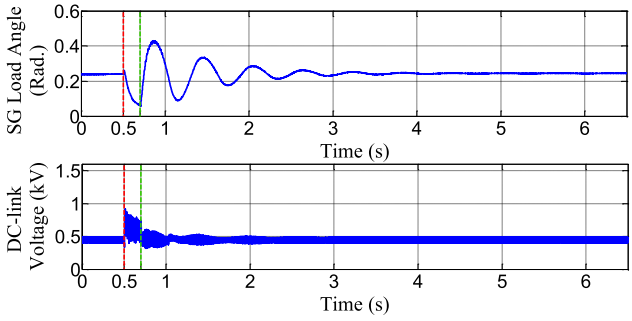

Fig. 16. SG load angle and dc-link voltage of the system of Fig. 14 containing VSG with alternating inertia.

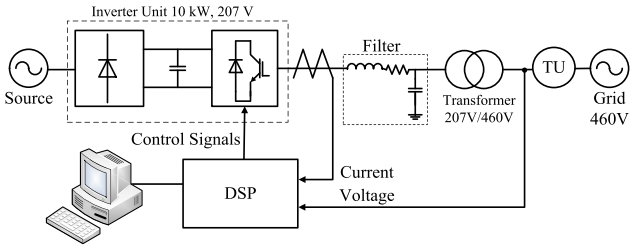

Fig. 17. Experimental system.

inertia scheme, and the severe transient of dc-link voltage was also eliminated.

VI. Experimental Results

The damping effect of alternating inertia was verified by applying to a laboratory-scale test system. The overall system configuration is shown in Fig. 17, and the main parameters of the system are presented in Table II. The transmission unit in Fig. 17 simulates the π model of a 40 km transmission line shown in Fig. 18.

Initially, the VSG with the constant moment of inertia $J = 0.563$ kgm^2 was subjected to a step change of 3 kW in the power reference. This value of J is calculated by assuming the inertia constant $H = 8$ s at rated power and frequency. The output power and angular velocity of the VSG is shown in Fig. 19. When the power reference increased, the VSG output power followed the power command after passing severe oscillations with the amplitude of 2 kW. The VSG stopped operating by applying 3.6 kW power command. Fig. 20 shows the RMS values of the VSG voltage and

TABLE II
SPECIFICATIONS OF THE EXPERIMENTAL SYSTEM

Base Power	10 kVA
Base Frequency	60 Hz
Switching Frequency	14 kHz
Dc-link Voltage	320 V
Filter Stray Resistance	0.23%
Filter Inductive Reactance	8.8%
Filter Capacitor VAR	1.62%
Resonance Frequency of LC Filter	1.59 kHz
Transformer Reactance	9.68%

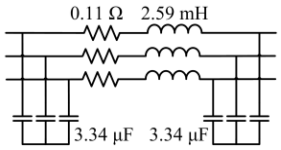

Fig. 18. π model of a 40 km transmission line.

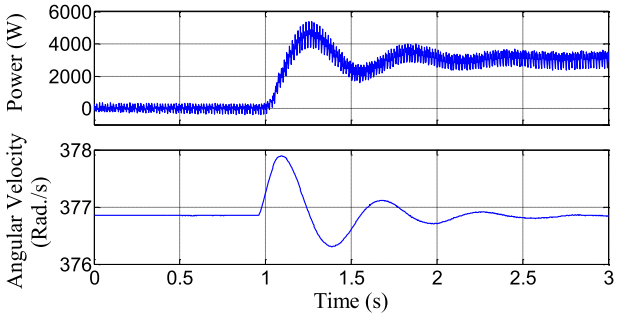

Fig. 19. Output power and virtual angular velocity of VSG with fixed moment of inertia of 0.563 kgm^2 and $D = 17$ pu.

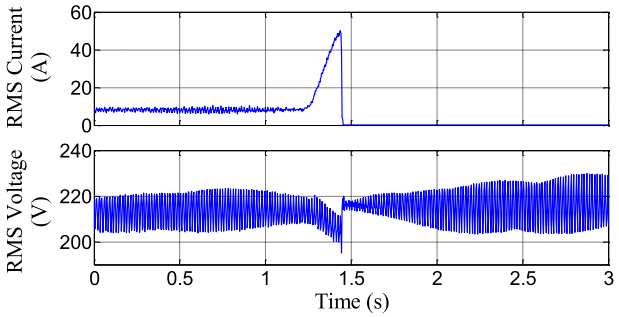

Fig. 20. RMS values of the VSG current and voltage with the fixed moment of inertia of 0.563 kgm^2 and $D = 17$ pu subjected to a 3.6 kW step power increase.

current in this condition. Because of the severe oscillation, the VSG current exceeded its tolerable limit and the inverter was stopped at $t = 1.43$ s.

Then, the VSG control was changed to the alternating inertia scheme with $J_{\text{big}} = 0.563$ kgm^2 and $J_{\text{small}} = 0.1$ kgm^2, and the step power change of 45 kW was applied. The result is shown in Fig. 21. It is observed that the VSG follows the power command without oscillations. It can be concluded that the VSG with alternating inertia can be loaded reliably at power levels close to its rating, and also can ride-through severer changes or disturbances. The effectiveness of the alternating inertia in the smooth transition of current level and

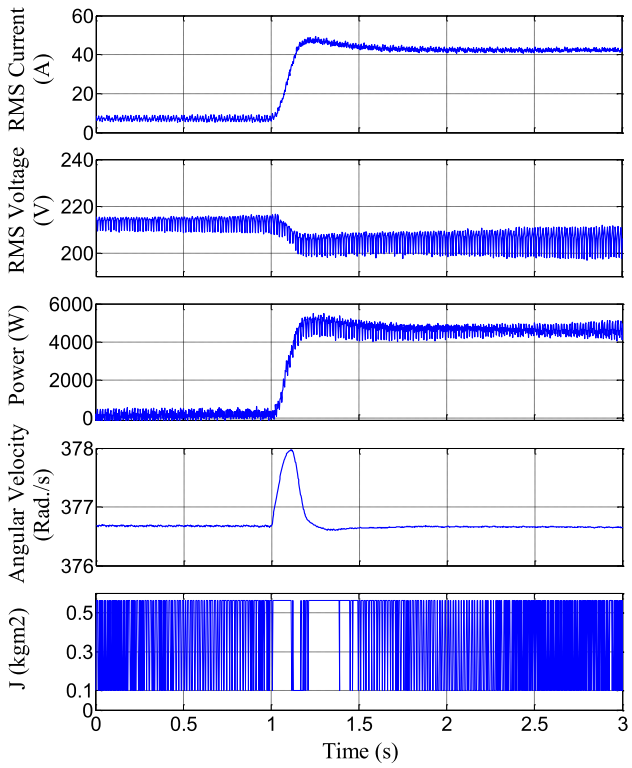

Fig. 21. RMS current, RMS voltage, output power, virtual angular velocity, and virtual moment of inertia of VSG with alternating J and $D = 17$ pu after a power command of 4.5 kW.

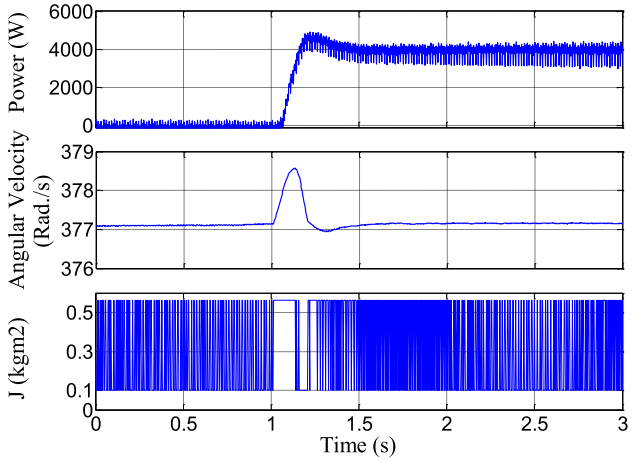

Fig. 22. Output power, virtual angular velocity, and moment of inertia of VSG with alternating J and $D = 0$ pu.

reducing the voltage ripples at the VSG terminal is obvious in this figure.

To clarify the damping effect of the alternating inertia scheme, the VSG with alternating inertia and zero damping factor D is subjected to a change of 3 kW in the power reference. It must be noted that the VSG with fixed inertia and zero damping factor cannot get into step with grid frequency and fails to track power reference after any disturbance. Output power, virtual angular velocity, and the real-time adopted J are shown in Fig. 22. As it is expected, the VSG can track the power reference with negligible transients.

VII. Conclusion

In this paper, the alternating inertia structure was elaborated. The alternating inertia scheme adopts the suitable value of the moment of inertia of the VSG considering its virtual angular velocity and acceleration/deceleration in each phase of oscillation. By selecting a big value for the moment of inertia during acceleration, the haste was mitigated, and on the other hand, during deceleration, a small value for inertia factor was adopted to increase the deceleration effect. The system transient energy analysis was used to assess the stabilizing effect of alternating inertia control. It was clarified by the energy analysis that the system transient energy is reduced promptly by the reduction in the value of the moment of inertia. Actually, in the case of a real synchronous machine, this transient energy is dissipated by damping terms during oscillations, whereas the alternating inertia control eliminates the transient energy directly and prevents its flow from dc storage and dissipation. Compared to normal damping factor D, the damping exerted by alternating inertia is considerably more effective and has identical results in any conditions. In addition, the transient energy can be reduced to zero at the end of the first quarter-cycle by alternating inertia control. Therefore, any transients can be eliminated before appearing. The idea does not only stabilize the VSG unit, but also enhances the stability of other machines in the system. Two configurations were assessed by simulation and the stabilizing effect of alternating inertia on the adjacent machines was illustrated. The proposed scheme was realized on the experimental system and the results affirmed the outstanding stabilizing effect of alternating inertia.

References

[1] Q.-C. Zhong and T. Hornik, *Control of Power Inverters in Renewable Energy and Smart Grid Integration*. New York, NY, USA: Wiley, 2013.

[2] L. Zhang, L. Harnefors, and H.-P. Nee, "Power-synchronization control of grid-connected voltage-source converters," *IEEE Trans. Power Syst.*, vol. 25, no. 2, pp. 809–820, May 2010.

[3] F. Blaabjerg, R. Teodorescu, M. Liserre, and A. V. Timbus, "Overview of control and grid synchronization for distributed power generation systems," *IEEE Trans. Ind. Electron.*, vol. 53, no. 5, pp. 1398–1409, Oct. 2006.

[4] Q.-C. Zhong, P.-L. Nguyen, Z. Ma, and W. Sheng, "Self-synchronized synchronverters: Inverters without a dedicated synchronization unit," *IEEE Trans. Power Electron.*, vol. 29, no. 2, pp. 617–630, Feb. 2014.

[5] J. Driesen and K. Visscher, "Virtual synchronous generators," in *Proc. IEEE Power Energy Soc. General Meeting-Convers. Del. Elect. Energy 21st Century*, Jul. 2008, pp. 1–3.

[6] T. Loix, S. De Breucker, P. Vanassche, J. Van den Keybus, J. Driesen, and K. Visscher, "Layout and performance of the power electronic converter platform for the VSYNC project," in *Proc. IEEE Powertech Conf.*, Jun./Jul. 2009, pp. 1–8.

[7] Q.-C. Zhong and G. Weiss, "Synchronverters: Inverters that mimic synchronous generators," *IEEE Trans. Ind. Electron.*, vol. 58, no. 4, pp. 1259–1267, Apr. 2011.

[8] M. P. N. van Wesenbeeck, S. W. H. de Haan, P. Varela, and K. Visscher, "Grid tied converter with virtual kinetic storage," in *Proc. IEEE Bucharest PowerTech*, Bucharest, Romania, Jun./Jul. 2009, pp. 1–7.

[9] M. Torres and L. A. C. Lopes, "Virtual synchronous generator control in autonomous wind-diesel power systems," in *Proc. IEEE Elect. Power Energy Conf. (EPEC)*, Montreal, QC, Canada, Oct. 2009, pp. 1–6.

[10] V. Karapanos, S. de Haan, and K. Zwetsloot, "Real time simulation of a power system with VSG hardware in the loop," in *Proc. 37th Annu. Conf. IEEE Ind. Electron. Soc. (IECON)*, Nov. 2011, pp. 3748–3754.

[11] R. Hesse, D. Turschner, and H.-P. Beck, "Micro grid stabilization using the virtual synchronous machine," in *Proc. Int. Conf. Renew. Energies Power Quality (ICREPQ)*, no. 472, pp. 1–6, Apr. 2009.

[12] Y. Xiang-Zhen, S. Jian-Hui, D. Ming, L. Jin-Wei, and D. Yan, "Control strategy for virtual synchronous generator in microgrid," in *Proc. 4th Int. Conf. Electr. Utility Deregulation Restruct. Power Technol. (DRPT)*, Jul. 2011, pp. 1633–1637.

[13] N. Soni, S. Doolla, and M. C. Chandorkar, "Improvement of transient response in microgrids using virtual inertia," *IEEE Trans. Power Del.*, vol. 28, no. 3, pp. 1830–1838, Jul. 2013.

[14] K. Sakimoto, Y. Miura, and T. Ise, "Stabilization of a power system with a distributed generator by a virtual synchronous generator function," in *Proc. IEEE 8th Int. Conf. Power Electron. ECCE Asia (ICPE & ECCE)*, May/Jun. 2011, pp. 1498–1505.

[15] J. Alipoor, Y. Miura, and T. Ise, "Evaluation of virtual synchronous generator (VSG) operation under different voltage sag conditions," in *Proc. IEE Jpn. Joint Tech. Meeting Power Eng. Power Syst. Eng.*, Tokyo, Japan, 2012, pp. 41–46.

[16] T. Shintai, Y. Miura, and T. Ise, "Reactive power control for load sharing with virtual synchronous generator control," in *Proc. Power Electron. Motion Control Conf. (IPEMC)*, Jun. 2012, pp. 846–853.

[17] J. Alipoor, Y. Miura, and T. Ise, "Distributed generation grid integration using virtual synchronous generator with adoptive virtual inertia," in *Proc. IEEE Energy Convers. Congr. Expo. (ECCE)*, Sep. 2013, pp. 4546–4552.

[18] J. Machowski, J. Bialek, and J. Bumby, *Power System Dynamics: Stability and Control*, 2nd ed. Chippenham, U.K.: Wiley, 2008, pp. 222–230.

Jaber Alipoor received the B.Sc. degree from the Department of Electrical Engineering, University of Mazandaran, Babolsar, Iran, in 2007, and the M.Sc. degree from the Department of Electrical Engineering, Shahed University, Tehran, Iran, in 2010. He is currently pursuing the Ph.D. degree with Osaka University, Suita, Japan.

His current research interests include power system stability, power quality, and distributed power generation.

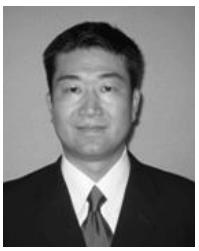

Yushi Miura received the Dr.Ing. degree in electrical and electronic engineering from the Tokyo Institute of Technology, Tokyo, Japan, in 1995.

He was with the Japan Atomic Energy Research Institute, Osaka University, Suita, Japan, from 1996 to 2004, where he is currently an Associate Professor with the Division of Electrical, Electronic, and Information Engineering. He is studying applications of power electronics to power systems.

Toshifumi Ise received the Dr.Ing. degree in electrical engineering from Osaka University, Suita, Japan, in 1986.

He is currently a Professor with the Division of Electrical, Electronic, and Information Engineering, Graduate School of Engineering, Osaka University. His current research interests include power electronics and applied superconductivity, including power quality issues, such as voltage sag compensator, superconducting magnetic energy storage, and new distribution systems, including many distributed generations.